

Landscape of s-triazine molecule on Si(100) by a theoretical x-ray photoelectron spectroscopy and x-ray absorption near-edge structure spectra study

Jing Hu(胡静), Xiu-Neng Song(宋秀能), Sheng-Yu Wang(王胜雨), Juan Lin(林娟), Jun-Rong Zhang(张俊荣), Yong Ma(马勇)

Citation: Chin. Phys. B . 2018, 27(11): 113101. **doi:** 10.1088/1674-1056/27/11/113101

Journal homepage: http://cpb.iphy.ac.cn; http://iopscience.iop.org/cpb

What follows is a list of articles you may be interested in

Laser cooling of CH molecule: Insights from *ab initio* study

Jie Cui(崔洁), Jian-Gang Xu(徐建刚), Jian-Xia Qi(祁建霞), Ge Dou(窦戈), Yun-Guang Zhang(张云光)
Chin. Phys. B . 2018, 27(10): 103101. **doi:** 10.1088/1674-1056/27/10/103101

Configuration interaction calculations on the spectroscopic and transition properties of magnesium chloride

Dong-lan Wu(伍冬兰), Cheng-quan Lin(林成泉), Yu-feng Wen(温玉锋), An-dong Xie(谢安东), Bing Yan(闫冰)
Chin. Phys. B . 2018, 27(8): 083101. **doi:** 10.1088/1674-1056/27/8/083101

First-principles study of solute diffusion in Ni_3Al

Shaohua Liu(刘少华), Zi Li(李孜), Chongyu Wang(王崇愚)
Chin. Phys. B . 2017, 26(9): 093102. **doi:** 10.1088/1674-1056/26/9/093102

Theoretical study of spin-forbidden cooling transitions of indium hydride using *ab initio* methods

Yun-Guang Zhang(张云光), Hua Zhang(张华), Ge Dou(窦戈)
Chin. Phys. B . 2017, 26(9): 093101. **doi:** 10.1088/1674-1056/26/9/093101

Responsive mechanism of three novel hypochlorous acid fluorescent probes and solvent effect on their sensing performance

Yong Zhou(周勇), Yun-Kun Wang(王云坤), Xiao-Fei Wang(王晓菲), Yu-Jin Zhang(张玉瑾), Chuan-Kui Wang(王传奎)
Chin. Phys. B . 2017, 26(8): 083102. **doi:** 10.1088/1674-1056/26/8/083102

Landscape of s-triazine molecule on Si(100) by a theoretical x-ray photoelectron spectroscopy and x-ray absorption near-edge structure spectra study*

Jing Hu(胡静), Xiu-Neng Song(宋秀能)†, Sheng-Yu Wang(王胜雨), Juan Lin(林娟), Jun-Rong Zhang(张俊荣), and Yong Ma(马勇)‡

School of Physics and Electronics, Shandong Normal University, Jinan 250014, *China*

(Received 3 August 2018; revised manuscript received 5 September 2018; published online 25 October 2018)

The chemisorbed structure for an aromatic molecule on a silicon surface plays an important part in promoting the development of organic semiconductor material science. The carbon K-shell x-ray photoelectron spectroscopy (XPS) and the x-ray absorption near-edge structure (XANES) spectra of the interfacial structure of an s-triazine molecule adsorbed on Si(100) surface have been performed by the first principles, and the landscape of the s-triazine molecule on Si(100) surface has been described in detail. Both the XPS and XANES spectra have shown their dependence on different structures for the pristine s-triazine molecule and its several possible adsorbed configurations. By comparison with the XPS spectra, the XANES spectra display the strongest structural dependency of all of the studied systems and thus could be well applied to identify the chemisorbed s-triazine derivatives. The exploration of spectral components originated from non-equivalent carbons in disparate local environments has also been implemented for both the XPS and XANES spectra of s-triazine adsorbed configurations.

Keywords: s-triazine, silicon surface, x-ray photoelectron spectroscopy (XPS), x-ray absorption near-edge structure (XANES)

PACS: 31.10.+z, 31.15.A–, 31.15.ag **DOI:** 10.1088/1674-1056/27/11/113101

1. Introduction

The research of adsorption for organic molecules on the surface of silicon has attracted widespread attention from the scientific community.[1–3] In recent years, the invention of nano- and molecule-size constructed devices has played a significant role in the development of material science. As an important functional material in various fields of science and technology, the application range of semiconductor silicon has gradually been expanded due to its excellent characteristics, and thus we have higher and higher requirements for its optical, thermal, electrical, and mechanical properties. After scientific research, it is found that the chemical modification of the silicon surface can improve its performance. Additionally, silicic technology and the manufacture of novel molecular electronic devices could be expanded through functionalization and modification of silicon surface, particularly in the case of ordered-layer controlled surface reactions. The functionalized realization of the silicon surfaces is applied in many fields, such as traditional electronics, microelectronics, and biosensing, to produce molecular complementary metal oxide semiconductor (CMOS) devices,[4,5] mixed molecular silicon storage capacitor structure,[5–7] bio-sensor, and so on. Because of the important properties and effects of this material, it is necessary to study and exploit this kind of chemical adsorbate. The approach of combing molecular function with traditional semiconductor technique could be performed directly by the strong covalent connection (Si–C covalent bonds) between organic molecules and silicon surfaces.[5,8] To manufacture the ideal organic material well, aromatic compounds could be a good choice for adsorbing on the silicon surface. Various structures have been produced by chemi-adsorption of an aromatic molecule on the silicon surface (Si(100)), and these structures are related to the size, polarity, types of heteroatoms, and substituent groups of aromatic rings.[5,9] The interaction between aromatic molecules and surfaces is complicated by the possibility of diverse bonding geometries. In aromatic molecules, the s-triazine molecule holding high symmetry may be ideal building blocks of constituting chemical compounds. So far, s-triazine molecule with the aromaticity in the traditional sense has been widely applied to produce herbicides,[10] fungicides, and medicinal chemistry.[11] The complexity of adsorption can be reduced owing to the high symmetry of s-triazine. Recently, the study on chemisorption of s-triazine molecule involving three N atoms on Si(100) surface is gradually being focused. According to previous related literature,[12] we construct five possible different adsorption configurations of s-triazine on Si(100). For the present, the landscape and identification of structures are two of the basic investigations for this kind of chemisorption systems,

*Project supported by the National Natural Science Foundation of China (Grant Nos. 11874242, 11804196, and 11804197).

†Corresponding author. E-mail: xiuneng@sdnu.edu.cn

‡Corresponding author. E-mail: mayong@sdnu.edu.cn

© 2018 Chinese Physical Society and IOP Publishing Ltd

which could conduce to a wider range of applications as organic semiconductors. The aim of this study is to discern the five possible chemisorption structures of s-triazine on Si(100) surface.

The electronic, vibrational, and geometric properties of organic semiconductors have been probed by common spectroscopic technologies, such as infrared (IR),[13] Raman spectra,[14–16] and soft x-ray spectroscopies,[17–20] which represent the single electron at core level is ionized outside or excited to a high level, and are believed to be extremely useful tools to efficiently investigate the electron-structure of matter by core-electron excitations/de-excitations. Among the soft x-ray spectroscopies, the x-ray photoelectron spectroscopy (XPS) and the x-ray absorption near-edge structure (XANES) spectrum are powerful technologies to explore interfacial structure of single or ordered monolayers adsorbed on surfaces.[1,21–26] The XPS describes the ionization of electrons at core level to display the chemical states of specific objects, while the XANES spectroscopy maps out characteristics of virtual orbitals. Historically, the XANES spectroscopies of small cluster models have been implemented theoretically for adsorbate of organic layers on Si(100) surface.[27–31] The current study focuses on five possible chemical adsorption structures, namely, Mode 1 (one C atom and one N atom in the para position of the s-triazine molecule with Si atoms on one dimer,[32] respectively, form a strong covalent bond Si–C and coordinate bond Si–N), Mode 2 (one C atom and one N atom in the adjacent position of the s-triazine molecule with the Si atoms on one dimer respectively form a strong covalent bond Si–C and coordinate bond Si–N), Mode 3 (two Si–C bonds and two Si–N dative bonds by addition across two adjacent dimers), Mode 4 (on the basis of Mode 3, the aromatic ring turns 90 degrees and continues to hold two Si–C bonds and two Si–N dative bonds in this configuration), and Mode 5 (the adsorbed s-triazine molecule is across two dimer rows). Finite-size clusters are used to accurately and effectively simulate the x-ray spectra of an s-triazine molecule on Si(100) in this work. We mainly show a systematic analysis and theoretical research of the XPS and XANES spectra at the carbon K-edge (1s) of these five structures at the density functional theory (DFT) level, which is gradient-corrected. The key intention of current work is to explore the connection between structural information and x-ray spectroscopy and verify the structural dependence of spectroscopy. This theoretical study of related adsorption structures of s-triazine on Si(100) surface through x-ray spectroscopy can promote and stimulate the development of both organic semiconductors and novel material devices in the future.

2. Calculation details

In our calculative strategy, we assumed the silicon surface to be an ideal surface and the triazine molecule was considered to be adsorbed on the Si(100) in five possible bonding modes. We chose finite clusters of suitable sizes which in different adsorbed modes contain, respectively, 17 Si atoms, 29 Si atoms, and 31 Si atoms for our calculations, and the silicon atoms of these five selected segments at the boundary were properly saturated with hydrogen atoms. The geometric optimizations of the selected clusters containing s-triazine molecule and finite Si atoms for the five possible adsorbed structures were carried out at the DFT level with B3LYP/6-31G(d,p) functional applying the Gaussian09 package.[33] Next, the C-1s XPS and XANES spectra of the five fully optimized structures were obtained through simulation by the StoBe program[34] with the DFT method. In these spectral computations, we chose the gradient-corrected Becke (BE88) exchange-functional[35] and the Perdew (PD86) correlation-functional[36] following the calculative process in previous studies about carbon-based systems and organic compounds,[23,37–42] which have been widely applied in our study and have been well aligned with the experiment. The IGLO-III (localized orbital) basis set[43] of triple-ζ quality individual gauge was utilized for the description of core-excited atom, and the TZVP (triple-ζ for valence-electrons plus polarization) basis set was used for other atoms, except for silicon atom which was described by DZVP (double-ζ for valence-electrons plus polarization). Miscellaneous auxiliary basis sets were used for all atoms and the equivalent nuclear potentials were set for the unexcited atoms to motivate the self-consistent-field (SCF) convergence. Specifically, the C-1s core ionic potentials (IPs) were calculated by the ΔKohn–Sham (ΔKS) scheme[44,45]

$$\mathrm{IP} = {}^{N-1}E_{\mathrm{FCH}} - {}^{N}E_{\mathrm{GS}}, \tag{1}$$

where the IP denotes the difference of energy between the ground-state (GS) and the full core hole (FCH) state (i.e., the optimized core-ionized state). Here, the exact ionization potentials could be obtained because of the consideration of relaxation led by the core hole state in the ΔKS approach. The C-1s XPS spectra of the five structures were evaluated through broadening by Gaussian line shape with full-width-at-half-maximum (FWHM) equal to 0.3 eV. As for the XANES spectral computations, the FCH approximation was adopted at DFT level. Meanwhile, the normal basis set was used for minimization of energy to facilitate the SCF mentioned above, and an addition of augmented diffuse basis set (19s, 19p, and 19d)[46] was carried out. There are two states in the absorption spectroscopy, the initial state (the ground state) and the final state (the core-excitation state). In terms of the final-state-rule,[47–50] the absorption spectroscopies could be calculated precisely by the wave-function of the core-excitation state for

the finite molecular systems. Thus, for the transition from the initial state i to the final state f, the intensity of absorption oscillator is given by[51]

$$O_{if} = \frac{2m\varepsilon_{if}}{3\hbar^2}(|\langle\psi_f|x|\psi_i\rangle|^2 + |\langle\psi_f|y|\psi_i\rangle|^2 + |\langle\psi_f|z|\psi_i\rangle|^2), \quad (2)$$

where O_{if} is the intensity of absorption oscillator, and ε_{if} represents the energy difference of the correlative orbitals. After evaluating the raw spectra with the FCH approximation which provides extremely good transition moments and exactly relative energy positions, the calibration of these spectra was performed by a ΔSCF scheme[44,45] to get absolute energy positions of the peaks, hence the energy of transition from the core orbital to the lowest unoccupied molecular orbital (LUMO) was calculated by

$$\varepsilon^{\Delta KS}_{1s\to LUMO} = {}^{N}E_{1s\to LUMO} - {}^{N}E_{GS}. \quad (3)$$

The transition energy of C-1s⟶LUMO is equal to the difference in energy between the two states; i.e., the GS and the majorized core-excited state in which one core electron was excited to LUMO. Then, the raw spectra aligned the first feature to the transition energy evaluated by ΔSCF. Below the IP range, the absorption oscillator strengths were convoluted by FWHM = 0.2 eV in a Gaussian function, while the cross section of photoionization was formed by the Stieltjes imaging approach[52–54] in the continuum range. Finally, in consideration of the relativistic effect, a uniform revision of 0.2 eV was added to the XPS or XANES spectra for the carbon element K-edge. In short, for the five chemisorption structures, first, we calculated the atomic stick spectra of the all nonequivalent carbons; next, each stick spectrum was broadened; and finally, the total spectra were obtained by the summation of contribution of each nonequivalent carbon atom.

3. Results and discussions

3.1. Geometric structures

The absorption of target molecule on Si(100) surface has only a few limited configurations due to the special symmetry of s-triazine. For s-triazine, the dative bond between an electronegative nitrogen atom and a silicon atom of the surface is shaped by a barrier-free process.[12] At low temperatures, it seems to be propitious to the formation of Si–N dative bonds. As suggested by the available experiment, the s-triazine molecule is parallel to the silicon surface when the adsorbed sample is heated to 200 K. In our work, the fully optimized geometries of both the s-triazine molecule and the five possible adsorbed derivatives are displayed in Fig. 1. It is worth pointing out that Mode 1 holds the butterfly shape. The five possible adsorbed structures could be divided into three types according to the number of bonds between the chemisorbed s-triazine and silicon surface, as well as their attended modes. As shown in Fig. 1, the first kind of configuration (i.e., Mode 1 and Mode 2) is adsorbed on the same silicon dimer, which leads to two on-dimer addition structures; namely, on-dimer butterfly (OD-BF) and on-dimer titled (OD-TL), respectively. The second kind of structure (i.e., Mode 3 and Mode 4) with two covalent Si–C bonds and two dative Si–N bonds saturating two adjacent-dimers on the same row causes two tight bridge (TB) structures which could be called TB_I and TB_{II}, respectively. Generally, the final type (Mode 5) is taken as cross-row bridge (CRB) structure which is formed by an s-triazine molecule straddling on two dimers in the same row. For convenience, in the following systematic discussion and comparison, these five conceivable adsorption structures are still represented by Mode 1, Mode 2, Mode 3, Mode 4, and Mode 5.

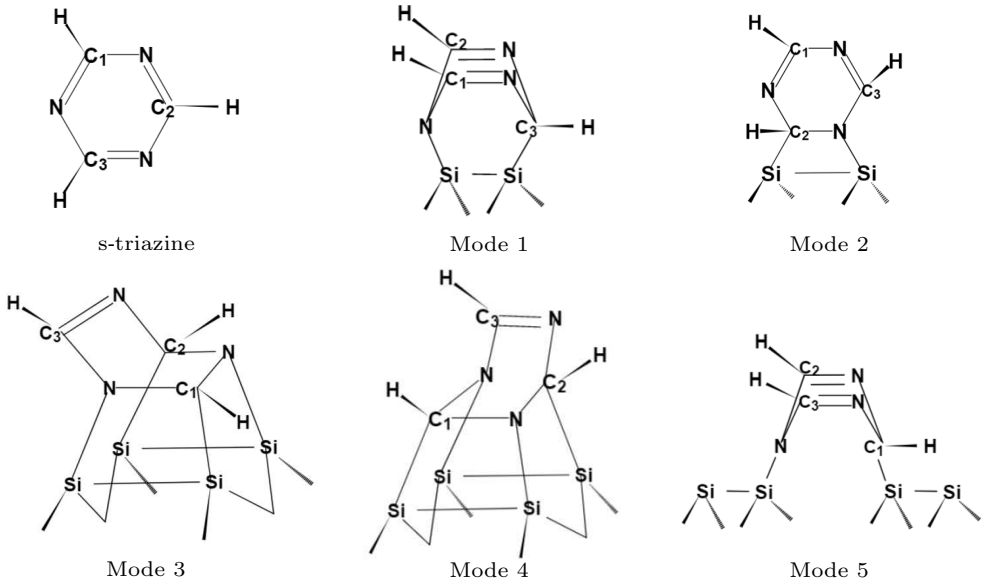


Fig. 1. The structures of s-triazine and its five typical chemisorbed configurations on Si(100).

To better investigate these five stable chemisorbed configurations, we also calculated their binding energies based on fully optimized molecular structures using DFT method (adsorption energies) by

$$E_{\rm ads} = E_{\rm st} + E_{\rm Si} - E_{\rm tot}, \tag{4}$$

where $E_{\rm ads}$ denotes the binding energy, which is evaluated as the difference between the total energy of the corresponding system prior to the adsorption of atoms ($E_{\rm st}+E_{\rm Si}$) and the total energy of the system after the adsorption of atoms ($E_{\rm tot}$). The binding energies of the five configurations are demonstrated in Table 1. For the first type, Mode 1 and Mode 2 have similar binding energies, since the latter is 1.62 kcal/mol lower than the former, which indicates that Mode 1 has higher chemical stability compared to Mode 2. As for the TB structure, Mode 4 displays higher binding energy than Mode 3 by 8.78 kcal/mol, so the chemisorbed structure of Mode 4 is more stable than Mode 3. With regard to Mode 5, it holds −11.92 kcal/mol which is much higher than the other four structures. Therefore, based on the calculated binding energies, the CRB structure is the most stable configuration among these five adsorbed modes. For the five species of s-triazine adsorbed on the surface of the silicon dimer, the chemical environment of each carbon atom in each structure is different except for Mode 1 and Mode 5; that is, there are three symmetry-independent carbon atoms in the two former type derivatives, while the Mode 5 possesses two kinds of carbons. For clear analysis, the three carbon atoms are separately marked as C_1, C_2, and C_3 in the following discussion. In Mode 1, the carbon atoms C_1 and C_2 are equivalent, the chemical environment of which is different from C_3. As for Mode 5, C_2 and C_3 are two equivalent carbon atoms, which are not equivalent to C_1.

Table 1. The binding energies of the five structures at DFT level.

Molecule	Binding energy/kcal·mol^{-1}
Mode 1	−22.74
Mode 2	−24.36
Mode 3	−58.50
Mode 4	−49.72
Mode 5	−11.92

3.2. C-1s XPS spectra

The C-1s XPS spectra of the s-triazine molecule and its five possible chemisorbed structures are shown in Fig. 2. Obviously, the two TB systems exhibit disparate XPS spectra in comparison with the two on-dimer structures and the only one CRB structure. The first type and the third type of configuration have two XPS spectral features *a* and *b*, while the TB structures only possess a feature *a*. Mode 1 and Mode 5 present similar C-1s XPS spectra not only on spectral profiles but also on energy coordinates of the main features. The peak *a* and peak *b* arise at about 290.63 eV and 291.156 eV in the photoelectron spectrum of Mode 1. As for Mode 5, its spectral features *a* and *b* are located at 290.4 eV and 291.11 eV, respectively. The relative intensities of the two characteristic peaks *a* and *b* in Mode 1 and Mode 5 are exactly opposite to that of Mode 2. Therefore, Mode 2 could be completely distinguished from Mode 1 and Mode 5 by sufficient XPS evidence. Moreover, Mode 3 and Mode 4 display roughly analogical C-1s XPS spectra. The two TB species show only one distinct spectral feature *a* at around 290.5 eV. One can see that C K-edge x-ray photoelectron spectra could not completely distinguish the five chemisorbed s-triazine species. Hence, the C-1s XPS spectra of the five structures of s-triazine adsorbed on Si(100) surface display distinct weak dependence on different structures so that the five structures could not be identified by XPS. To better reflect the relationship between structure and spectrum, we also plot pristine s-triazine molecule at the DFT level in Fig. 2. In the C-1s XPS spectra, one distinct feature *a* situated in the lowest energy in the pristine triazine molecule is different from the five chemisorbed s-triazine derivatives in spectral position and intensity. Compared to the primitive molecule, the five adsorbed derivatives exhibit an obvious red shift of about 2 eV; that is, the carbon atoms in primitive s-triazine hold higher K-edge IPs than the carbon atoms in chemisorbed derivatives, which reflects a charge transfer from Si(100) to the carbon atom of s-triazine during the adsorption caused by the non-metallic action between carbon and silicon under the silicon surface dimer.

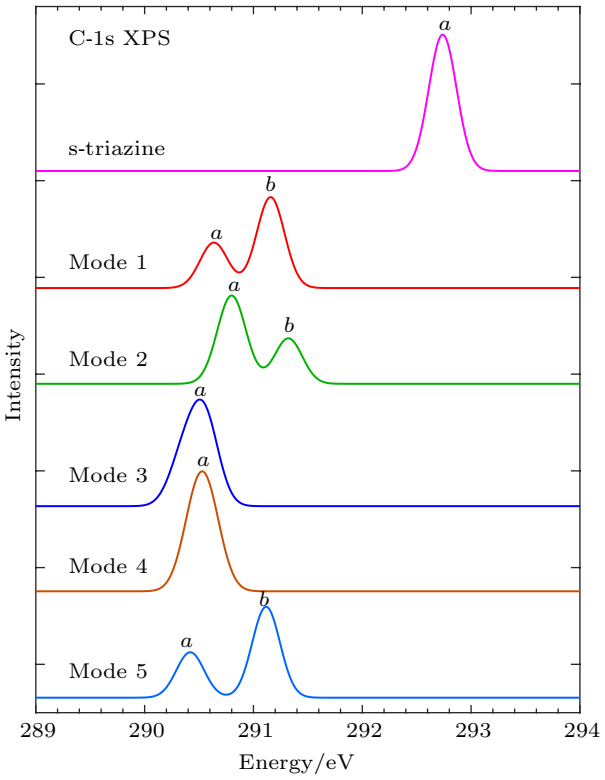


Fig. 2. (color online) Calculated C-1s XPS spectra of the five configurations of an s-triazine adsorbed on Si(100).

For further study of the spectral source on the five chemisorbed structures, we also calculated the specific spectra of unequal carbon atoms in each adsorbed configuration using above-mentioned measure method. The total C-1s XPS spectra of all the studied structures and the corresponding spectral components generated by non-equivalent carbons in each structure are displayed in Fig. 3. Herein, the carbon atoms of different local structures making contributions to the x-ray photoelectron spectra can be expounded for our studied systems. It is clearly observed that the first XPS spectral feature at the lowest energy in each adsorbed derivative benefits from the carbons bonded with silicon of the surface dimer. Specifically, feature *a* in Mode 1 and Mode 2 originates from C_3 and C_2, respectively, both of which are saturated by silicon atoms and electronegative nitrogen atoms simultaneously. The only one characteristic peak *a* in Mode 3 and Mode 4 comes mainly from the C_1 and C_2, and these two types of carbon atoms are connected to silicon atoms of the surface dimer in the two TB structures. As for Mode 5, its feature *a* is generated by C_1 bonded with silicon. In addition, the ionization value of carbon atoms not forming a covalent bond with silicon atoms are generally lower than that of carbons in the original s-triazine. It is notable that C_1 and C_2 produce somewhat similar spectral contributions while their local environments are different. In the meantime, these differences reflect changes of the electronic structure of the carbons for the s-triazine after adsorption. Our calculations not only show that the differences in IPs of carbon atoms are attributed to their different chemical environments, but also indicate that it is difficult to use XPS spectra for the identification of these five adsorbates. To fully distinguish the adsorbed s-triazines, the calculated XANES spectra are applied to further explore the relationship between structures and spectra in the next section.

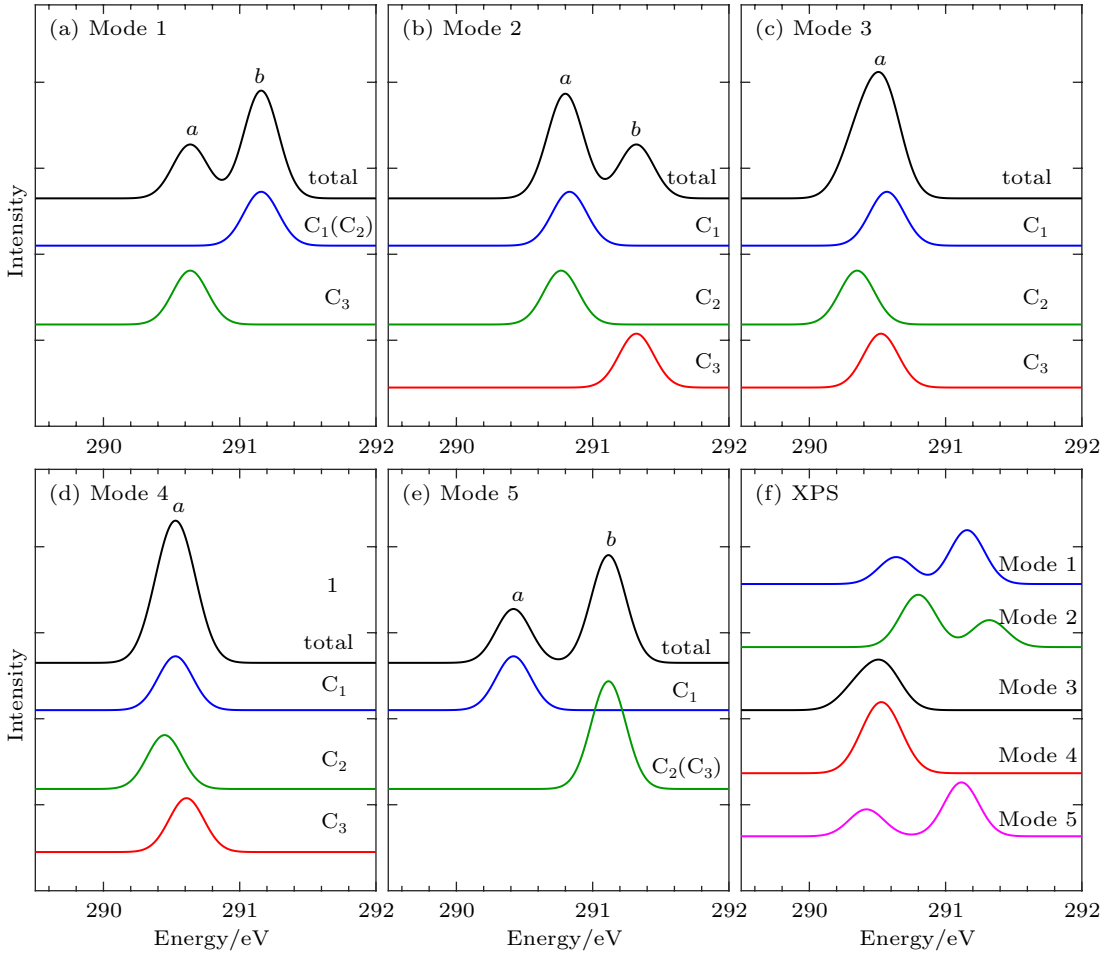


Fig. 3. (color online) Calculated C-1s XPS spectra of the five configurations of an s-triazine on Si(100), as well as spectral components corresponding to non-equivalent carbon atoms.

3.3. C-1s XANES spectra

The calculated C-1s XANES spectra of the s-triazine molecule and its five conceivable chemisorbed derivatives are displayed in Fig. 4. Visibly, the five s-triazine derivatives produce markedly distinctive XANES spectra, which is reflected in spectral profiles and energy positions of the corresponding peaks. To effectively identify these five structures, we only need to employ the spectral characteristics in the energy range of 285 eV–288 eV to achieve our study. Here, the excitation

energies of the main spectral feature for s-triazine molecule and its five derivatives are summarized in Table 2. In the XANES spectrum of Mode 5, the energy position of the first feature *a* (at about 286.1 eV) is much higher than the other four derivatives (from 285.55 eV to 285.84 eV), and in the energy region of 285 eV–288 eV, the CRB structure only has two distinct spectral features *a* and *b*, which is also different from the other four species. In comparison with the other three species, Mode 2 presents a notably different spectral profile, i.e., in its absorption spectrum, the relative intensities of peak *a* and peak *b* are opposite to those of the other three configurations. Therefore, Mode 2 could be readily identified from the remaining four possible adsorbed modes based on its distinguished XANES spectral characteristics. In the absorption spectrum of Mode 1, one distinct feature *a* emerges at around 285.67 eV, the intensity of which is much stronger than Mode 3 and Mode 4. Moreover, the spectral peaks *b* and *c* have almost the same intensity in Mode 1, while in the spectra of Mode 3 and Mode 4, the intensity of peak *b* is obviously stronger than peak *c*. The above discussion could be a powerful evidence to distinguish Mode 1 from the latter two structures by the C-1s XANES spectroscopy. Since the characteristics of Mode 3 and Mode 4 belong to the second type of TB structure, they not only have roughly the same XPS but also have some similarities in their absorption spectra. However, there is something different between the two configurations in their C-1s XANES spectra, which may be helpful to distinguish the two conformations. It is noted that Mode 4 exhibits an energy interval of about 0.6 eV between feature *c* and feature *d* (at about 287.19 eV and 287.79 eV, respectively), which is larger than 0.45 eV for Mode 3 in its corresponding energy range. In addition, in the spectrum of Mode 3, the relative intensities of peak *c* and peak *d* are clearly different from those in Mode 4, viz, they are exactly the opposite. In other words, the five chemisorbed s-triazine configurations could be identified well by the distinguishable C-1s XANES spectra. To understand the spectral changes after the adsorption of s-triazine, figure 4 also shows the C-1s XANES spectrum of the original s-triazine compared to these five adsorbed s-triazine structures. The primordial s-triazine presents a more concise XANES spectrum with three main spectral features *a*, *h*, and *i* at around 285.67 eV, 290.7 eV, and 291.4 eV, respectively. The pristine s-triazine possesses a relatively strong first absorption feature *a* than the ones (at about 285.54 eV–285.84 eV) in its five derivatives. Especially, the main absorption features (features *a* and *b*) of the five adsorption configurations shift to higher energies compared to pristine s-triazine molecule, which shows the increase of the energy difference between the core level and unoccupied state. Furthermore, the peaks *h* and *i* of the s-triazine appear at higher energy position than those of the five configurations (peak *h*, 289.4 eV–289.9 eV; peak *i*, 289.8 eV–290.3 eV). Thus, it can be seen that all the studied systems could be differentiated from each other by applying the C-1s x-ray absorption spectroscopies. Meanwhile, the five chemisorption structures have different XANES spectra as compared to the pristine s-triazine.

Table 2. The excited energies (eV) of significant spectral peaks for C-1s XANES spectra of s-triazine and its five chemisorbed structures.

Molecules	*a*	*b*	*c*	*d*	*h*	*i*
s-triazine	285.67	–	–	–	290.7	291.4
Mode 1	285.84	286.7	287	287.9	289.89	290.29
Mode 2	285.54	285.89	286.59	287	289.6	289.89
Mode 3	285.8	286.4	287	287.45	289.4	289.8
Mode 4	285.69	286.49	287.19	287.79	289.3	289.64
Mode 5	286.1	287	–	–	289.64	290.2

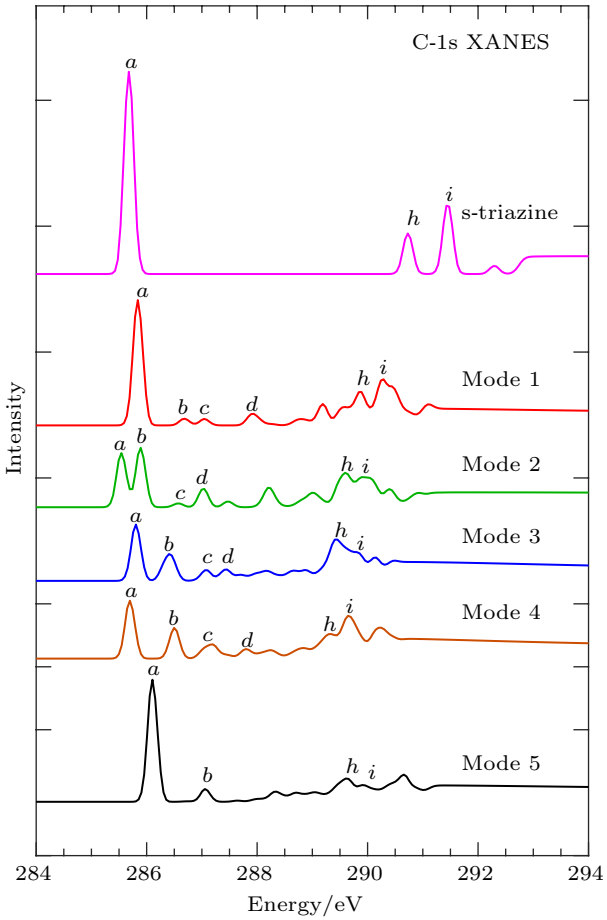


Fig. 4. (color online) Calculated C-1s XANES spectra of the five configurations of s-triazine adsorbed on Si(100).

Figure 5 demonstrates the C-1s XANES spectra of the five interface structures of s-triazine adsorbed on Si(100) surface and spectral compositions produced by non-equivalent carbon atoms in different local environments. The first adsorbed characteristic *a* originates from C_1 and C_2 in Mode 1, and C_1 and C_3 in Mode 2; while in both Mode 3 and Mode 4, C_3 makes a contribution to the first feature *a*. With regard to Mode 5, its feature *a* is generated by C_2. It can be observed

that the absorption spectral peaks at the lowest energy region are generated by the carbon atoms bonded with nitrogen and hydrogen. The excitation energies of carbons connected to the silicon atoms in the five adsorbed structures occur at higher energy range than other carbons. Additionally, the intensities of peaks at higher energy region coming from the carbons saturated by silicon atoms in the surface dimer are weaker than those contributed by other carbons.

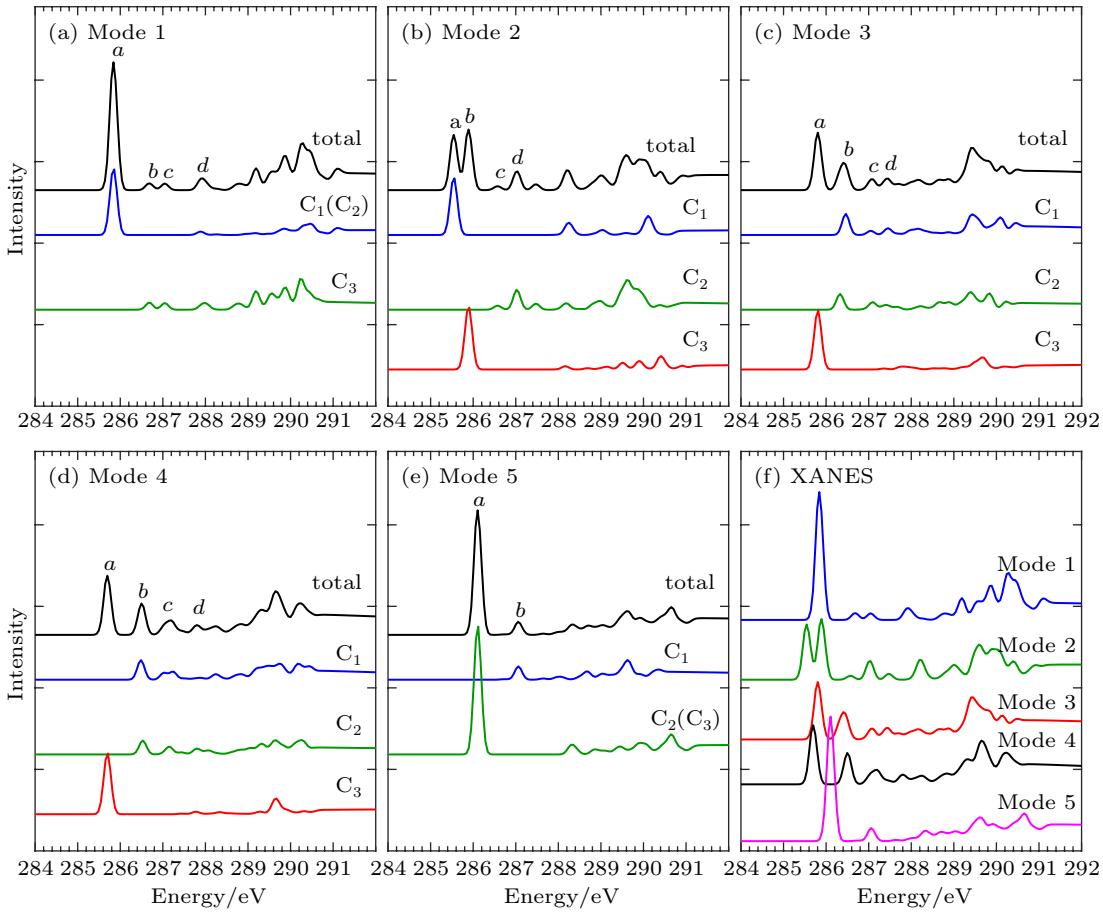


Fig. 5. (color online) Calculated C-1s XANES spectra of the five structures of s-triazine on Si(100) and their decompositions based on symmetry-independent carbons.

4. Conclusion

In summary, we have theoretically investigated the landscape of an s-triazine molecule adsorbed on Si(100) surface by the C-1s XPS and XANES spectroscopies with the DFT approach. The XPS and XANES spectra of the five configurations exhibit remarkable structural diversities on spectral features as compared to the original s-triazine. The XPS spectra do not absolutely display structural dependence to distinguish all the studied species. However, the apparent structural dependence is shown by the XANES spectra, so that the C-1s absorption spectra could be competent to distinguish the five adsorbed s-triazine derivatives from each other. Furthermore, the decompositions of the total spectra for the XPS and XANES of these derivatives have also been explored to illuminate the origin of spectral features. The carbons bonded with the silicon on the surface dimer have lower IPs than those in others for the XPS spectra. For the XANES spectra, the carbons connected to silicon exhibit higher excitation energies than others.

Acknowledgement

The support provided by China Scholarship Council (CSC) during a visit of Yong Ma to Royal Institute of Technology (KTH) is acknowledged. Thanks to the support of the Taishan Scholar Project of Shandong Province, China.

References

[1] Romeo M, Balducci G, Stener M and Fronzoni G 2014 *Surf. Sci.* **118** 1049
[2] Filler M A and Bent S F 2003 *Prog. Surf. Sci.* **73** 1
[3] Bent S F 2002 *Surf. Sci.* **500** 879
[4] Cummings S P, Savchenko J and Ren T 2011 *Coord. Chem. Rev.* **255** 1587
[5] O'Donnell K M, Warschkow O, Suleman A, Fahy A, Thomsen L and Schofield S R 2015 *Coord. Chem. Rev.* **27** 054002
[6] Wakayama Y and Hayakawa R 2014 *Thin Solid Films* **554** 2
[7] Shan T P, Buckley J, Huang K, Calborean A and Gély M, Delapierre G, Duclairoir G F, Marchon J C, Jalaguier E, Maldivi P, Salvo B D and Deleonibus S 2009 *IEEE Trans. Nanotechnol.* **8** 204

[8] Wolkow R A 1999 *Annu. Rev. Phys. Chem.* **50** 413
[9] Feng T and Bernasek S L and Guo Q X 2009 *Chem. Rev.* **109** 3991
[10] Krutz L J, Shaner D L, Weaver M A, Webb R M, Zablotowicz R M, Reddy K N, Huang Y B and Thomson S J 2010 *Pest Manag Sci* **66** 461
[11] Lim F P L and Dolzhenko A V2014 *Eur. J. Med. Chem.* **85** 371
[12] Ng W K H, Liu J W and Liu Z F 2015 *Phys. Chem. Chem. Phys.* **17** 16876
[13] Wang Q Q, Li P, Gao T, Wang H Y and Ao B Y 2016 *Chin. Phys. B* **25** 063102
[14] Paukshtis E A, Soltanov R I and Yurchenko E N 1981 *React. Kinet. Catal. Lett.* **16** 93
[15] Hayashi S and Ohmine I 2000 *J. Phys. Chem. B* **104** 10678
[16] Fleischmann M, Hendra P J and McQuillan A J 1974 *Chem. Phys. Lett.* **26** 163
[17] Castner D G, Hinds K and Grainger D W 1996 *Langmuir* **12** 5083
[18] Ishida T, Hara M, Kojima I, Tsuneda S, Nishida N, Sasabe H and Knoll W 1998 *Langmuir* **14** 2092
[19] Zhang H C, Liu H, Qiao W Q, Li X J, He S Y and Abraimof V V 2012 *Acta Phys. Sin* **61** 034213 (in Chinese)
[20] Yan Z X 2011 *Acta Phys. Sin* **60** 076202 (in Chinese)
[21] Luo C X, Xia H P, Yu C and Xu J 2011 *Acta Phys. Sin* **60** 077806 (in Chinese)
[22] Gao M, Du H W, Yang J, Zhao L, Xu J and Ma Z Q 2017 *Chin. Phys. B* **26** 045201
[23] Ma Y, Wang S Y, Hu J, Song X N, Zhou Y and Wang C K 2018 *Mater. Chem. Phys.* **207** 309
[24] Song X N, Hu J, Wang S Y, Ma Y, Zhou Y and Wang C K 2017 *Phys. Chem. Chem. Phys.* **19** 32647
[25] Ma Y, Wang S Y, Hu J, Zhou Y, Song X N and Wang C K 2018 *J. Phys. Chem. A* **122** 1019
[26] Ma Y, Wang S Y, Hu J, Zhang J R, Lin J, Yang S Q and Song X N 2018 *J. Phys. Chem. A* **122** 4750
[27] Bournel F, Carniato S, Dufour G, Gallet J J, Ilakovac V, Rangan S, Rochet F and Sirotti F 2006 *Phys. Rev. B* **73** 125345
[28] Besley N A and Blundy A J 2006 *J. Phys. Chem. B* **110** 1701
[29] Besley N A and Noble A 2007 *J. Phys. Chem. C* **111** 3333
[30] Carniato S, Rochet F, Gallet J J, Bournel F, Dufour G, Mathieu C and Rangan S 2007 *Surf. Sci.* **601** 5515
[31] Carniato S, Rochet F, Gallet J J, Bournel F, Dufour G, Mathieu C and Rangan S 2009 *Surf. Sci.* **603** 158
[32] Ng W K H, Liu J W and Liu Z F 2013 *J. Phys. Chem. C* **117** 26644
[33] http://gaussian.com/g09citation/
[34] http://www.fhi-berlin.mpg.de/KHsoftware/StoBe/whatsnew.html
[35] Becke A D 1988 *Phys. Rev. A* **38** 3098
[36] Perdew J P 1986 *Phys. Rev. B* **33** 8822
[37] Gao B, Liu L, Wang C R, Wu Z Y and Luo Y 2007 *J. Chem. Phys.* **127** 164314
[38] Song X N, Ma Y, Wang C K, Dietrich P M, Unger W E S and Luo Y 2012 *J. Phys. Chem. C* **116** 12649
[39] Song X N, Ma Y, Wang C K and Luo Y 2011 *Chem. Phys. Lett.* **517** 199
[40] Song X N, Wang G W, Ma Y, Jiang S Z, Yue W W, Wang C K and Luo Y 2016 *J. Phys. Chem. A* **120** 9932
[41] Song X N, Wang G W, Ma Y, Jiang S Z, Yue W W, Xu S C and Wang C K 2016 *Chem. Phys. Lett.* **645** 164
[42] Wang G W, Ma Y, Song X N, Jiang S Z, Yue W W, Wang C K and Luo Y 2016 *J. Phys. Chem. C* **120** 13779
[43] Kutzelnigg W, Fleischer U and Schindler M 1990 *NMR Basic Principles and Progress* (Berlin: Springer-Verlag) Vol. 23, p. 165
[44] Bagus P S 1965 *Phys. Rev.* **139** A619
[45] Triguero L, Plashkevych O, Pettersson L G M and Ågren H 1999 *J. Electron Spectrosc. Relat. Phenom.* **104** 195
[46] Triguero L, Pettersson L G M and Ågren H 1998 *Phys. Rev. B* **58** 8097
[47] Barth U V and Grossmann G 1979 *Solid State Commun.* **32** 645
[48] Barth U V and Grossmann G 1982 *Phys. Rev. B* **25** 5150
[49] Privalov T, Gel'mukhanov F and Ågren H 2001 *Phys. Rev. B* **64** 165116
[50] Privalov T, Gel'mukhanov F and Ågren H 2001 *Phys. Rev. B* **64** 165115
[51] Stöhr J 1992 *NEXAFS Spectroscopy* (Berlin: Springer Verlag)
[52] Langhoff P W and Corcoran C T 1974 *J. Chem. Phys.* **61** 146
[53] Langhoff P W, Corcoran C T, Sims J S, Weinhold F and Glover R M 1976 *Phys. Rev. A* **14** 1042
[54] Langhoff P W 1979 *Electron-Molecule and Photon-Molecule Collisions* (Rescigno T, McKoy V and Schneider B, Ed.) (Boston: Springer) pp. 183–224